OPEN ACCESS
Journal of Innovative Optical Health Sciences
Vol. 16, No. 5 (2023) 2241005 (8 pages)

DOI: 10.1142/S179354582241005X

World Scientific
www.worldscientific.com

Compact and robust dual-color linearly polarized illumination source for three-photon fluorescence imaging

Jiazheng Song*, Yanyan Zhang and Yuanshan Liu
School of Artificial Intelligence
Optics and Electronics (iOPEN)
Northwestern Polytechnical University
Xi'an, Shaanxi 710072, P. R. China
**songjiazheng@nwpu.edu.cn*

Received 15 May 2023
Accepted 8 June 2023
Published 22 July 2023

The miniaturized femtosecond laser in near infrared-II region is the core equipment of three-photon microscopy. In this paper, we design a compact and robust illumination source that emits dual-color linearly polarized light for three-photon microscopy. Based on an all-polarization-maintaining passive mode-locked fiber laser, we shift the center wavelength of the pulses to the 1.7 μm band utilizing cascade Raman effect, thereby generate dual-wavelength pulses. To enhance clarity, the two wavelengths are separated through the graded-index multimode fiber. Then we obtain the dual-pulse sequences with 1639.4 nm and 1683.7 nm wavelengths, 920 fs pulse duration, and 23.75 MHz pulse repetition rate. The average power of the signal is 53.64 mW, corresponding to a single pulse energy of 2.25 nJ. This illumination source can be further amplified and compressed for three-photon fluorescence imaging, especially dual-color three-photon fluorescence imaging, making it an ideal option for biomedical applications.

Keywords: Three-photon fluorescence imaging; illumination source; dual-wavelength femtosecond pulse; cascaded Raman effect; graded-index multimode fiber.

1. Introduction

Fluorescence microscopy has greatly promoted the development of biological science and medicine. By labeling structures with fluorescent dyes, fluorescence microscopy allows for high-resolution imaging of cellular and subcellular structures.[1–7] To achieve high-resolution three-dimensional functional imaging of living deep tissues, dye molecules are excited to emit fluorescence by absorbing multiple near-infrared photons, enabling three-dimensional imaging of deep tissues. In 1990, Denk *et al.* introduced the multiphoton absorption effect into laser scanning microscopy and invented the two-photon laser scanning microscope, which has rapidly accelerated the development of the multiphoton fluorescence imaging technology in living biological structures.[1]

*Corresponding author.

Two-photon and three-photon microscopies are currently the most commonly used methods in biological imaging, in which the illumination source plays a crucial role. Three-photon fluorescence imaging typically uses a 1.7 μm wavelength femtosecond laser as the illumination source, which has higher transmittance and smaller scattering effects and therefore can image biological tissues at a deeper level.[3,4] Additionally, the illumination source with dual-wavelength enables the dual-color imaging of biological tissues, which provides a more comprehensive and detailed visualization of their information, such as the spatial distribution[7,9] or the blood flow speed distribution.[8] For example, through a home-designed dual-wavelength femtosecond laser, Guesmi *et al.* performed the two-color three-photon images of fixed mouse brains and in live developing spinal cord explants, and obtained simultaneous three-photon fluorescence imaging of various combinations of GFPs and RFPs with superior contrast at large depths.[7] Besides, based on multiphoton microscopy with dual-wavelength signals, the measurement of the blood flow velocity of venules and arterioles in mouse brain *in vivo* has been reported.[8] Based on the dual-wavelength line-scan third harmonic generation (THG) imaging technology with optical pulses of 1680 nm and 1780 nm wavelengths, the researchers find that the blood flow speed has a distribution of rapid flow in the middle and slow flow on both sides, and the instantaneous blood flow velocity is not symmetric under general conditions. These results prove the dual-wavelength lasers are crucial for applicability in specific biological applications.

So far, there are various approaches to generate 1.7 μm pulses for fluorescence imaging, including directly generation,[10–12] Raman self-frequency shift,[13–17] supercontinuum generation,[18,19] and fiber parametric amplification.[20,21] The generation of signals around 1.7 μm from Bismuth-doped fiber and Thulium/Holmium co-doped fiber has been proposed, and signals with less than 1 ps pulse widths and over 1 nJ pulse energies have been obtained.[10,11] However, most of the components require customization, which makes this technique less commonly adopted. The intra-pulse stimulated Raman scattering (SRS) is the most commonly used method to generate soliton pulses at 1.7 μm,[13–17] but the energy of the Raman solitons is limited by the small effective mode area of the single mode fiber, which can be overcome with the use of very-large-mode-area (VLMA) fibers for high energy.[16] Additionally, a Raman fiber laser that combines the SRS gain and the thulium-fiber-based active gain has been demonstrated, reducing the lasing threshold, and improving the optical efficiency.[17] Supercontinuum generation can also produce spectra covering the 1.7 μm wavelength band, but its low-conversion efficiency makes it a rarely-used method.[18,19] In addition to the aforementioned methods, fiber optical parametric chirped pulse amplifier (FOPCPA) has been applied to generate 1.7 μm pulses.[20–22] FOPCPA-based all-fiber high-power lasers have the advantage of increasing the pulse energy to the mJ-level, however, its complex design, expensive components and high technical difficulty limit its widespread application.[22]

Despite the widespread coverage of researches on 1.7 μm lasers for three-photon microscopy, there are several issues that hinder its promotion. The high cost of commercial high-energy femtosecond lasers remains a significant challenge, which limits the accessibility of three-photon microscope for researchers. Additionally, although high-energy fiber lasers have been developed, they only output pulses with single wavelength, hampering the conduct of two-color three-photon microscopy researches, while dual-wavelength femtosecond pulses can achieve dual-color bioimaging.

Compared to the previously mentioned technologies, we have overcome the shortcomings of system complexity and high cost, and built a dual-wavelength dual-pulse illumination source with commonly used commercial components. This source has a compact, robust, and efficient structure with the dimensions of 24 cm $\times$ 12 cm $\times$ 45 cm, which makes it highly portable and more convenient for applications. Our source generates linearly polarized multiple pulses with multiple wavelengths based on cascaded Raman effects. We utilize the weak nonlinear effects of graded-index multimode fibers (GRIN MMFs) to achieve spectral separation of the multiple pulses. This allows the laser to produce dual-pulse sequences at 1639.4 nm and 1683.7 nm with 920 fs pulse width, and 23.75 MHz pulse repetition rate. The average power of the pulses is 53.64 mW, corresponding to a single pulse energy of 2.25 nJ, which can be further increased for fluorescence excitation. This illumination source enables researchers to conduct more detailed and advanced imaging of biological tissues. Additionally, this source is also suitable for label-free measurement

of blood flow velocity with dual-wavelength line-scan THG imaging technology. Overall, the illumination source presented here represents a new opportunity for biological imaging, and has high practical value and widespread implications for the field of biomedical optics.

2. Materials and Methods

The experimental setup is schematically presented in Fig. 1(a). The illumination source consists of a SESAM-based passively mode-locked fiber laser, which generates soliton pulses. The soliton pulses are initially directed into a pre-amplifier, utilizing an 80 cm EDF (Er80-8/125-PM, nLight Inc. USA) as the gain media. The PMWDM1 combines the 976 nm pump light with the soliton pulses into the EDF. After pre-amplification, the pulses pass through a PM isolator to eliminate the influence of unabsorbed pump light. Then, the pulses are injected into the main amplifier, consisting of a 3 m DCEY (DCF-EY-10/128-PM, CorActive High-Tech Inc. Canada), a PMMPC, a PMWDM2, and a 9 W multimode pump. The pulses are coupled into the DCEY fiber through the PMMPC along with high-power 976 nm pump light. Due to the high pump power and long DCEY length, the amplified pulses have a high peak power, making the PM isolator unsuitable for preventing the excess pump light. Therefore, PMWDM2 is adopted to separate the pump light from the amplified pulses. During the high power amplification, the high power pulses experience Raman frequency shift, resulting in the cascaded Raman solitons. A GRIN MMF is utilized to clearly separate the Raman peaks, and PMWDM3 is used to select the Raman solitons with longer wavelength. The pictures of the laser are depicted in Fig. 1(b), which has a compact and robust packaged footprint of 24 cm× 12 cm× 45 cm. The miniaturized structure of the laser increases its portability and makes it more convenient in bioimaging experiments. Finally, the dual-wavelength pulses are analyzed using an optical spectrum analyzer (AQ6375, Yokogawa Inc. Japan), an autocorrelator (PulseCheck 50, APE GmbH Germany), and a signal & spectrum analyzer (FSW26, Rohde & Schwarz Germany).

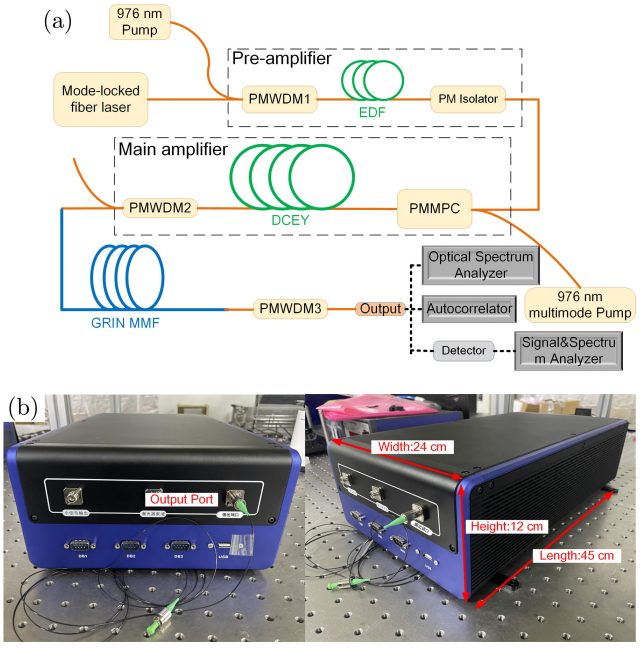

Fig. 1. (a) The schematic illustration of the experimental setup. PMWDM1, PMWDM2, PMWDM3: Polarization-maintaining wavelength division multiplexers, PMMPC: PM Pump & Signal Combiner, EDF: Er-doped fiber, DCEY: Dual-cladding Er:Yb co-doped fiber, GRIN MMF: Graded-index multimode fiber. (b) The pictures of the dual-color linearly polarized illumination source.

3. Results

Although the optical pulses with 1.7 μm wavelength are a good choice for three-photon fluorescence imaging as illumination source, it is not easy to directly generate due to the lack of traditional high-gain media for this wavelength band. The commonly used approach is to generate 1.55 μm femtosecond pulses based on the passively mode-locking techniques, and then shift the wavelength to the 1.7 μm band through the intrapulse Raman shift. The intrapulse Raman shift refers to the low-frequency components that are continuously amplified by the high-frequency components within the pulse through the Raman amplification, thereby the wavelength shift of the pulses towards a longer wavelength is realized, which is currently the simplest and most effective technique for frequency shift. In this work, we first output the 1.55 μm seed pulses through a self-made passively mode-locked fiber laser, and then pre-amplify them to increase the amplification efficiency of the main amplifier. When the pre-amplified pulses propagate in the main amplifier, the pulse energies are significantly increased, accompanied by the Raman frequency shift. As the pulse energy increases, cascaded Raman solitons with different wavelengths appear.

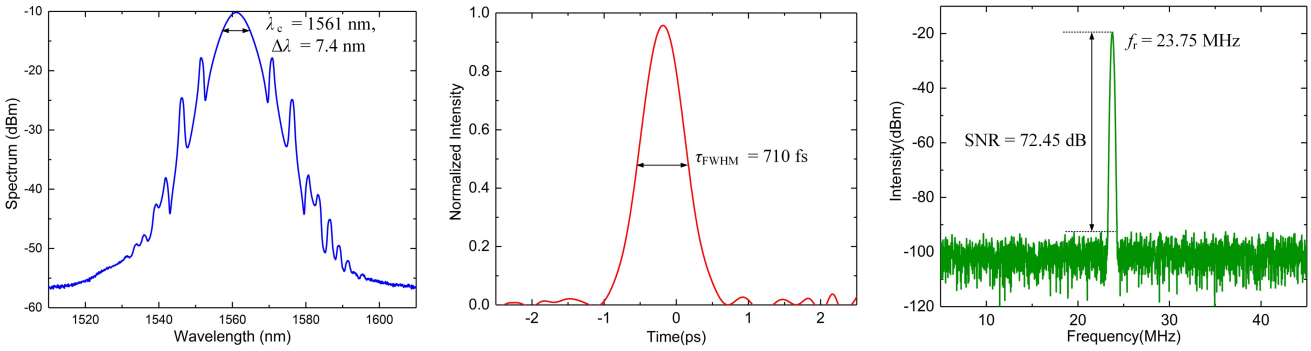

(a) (b) (c)

Fig. 2. The parameters of pulses directly from the mode-locked fiber laser. (a) Optical spectrum. (b) Intensity autocorrelation curve. (c) RF spectrum with 50 MHz span.

At this time, the wavelength separation of the cascaded Raman solitons is not very clear, then a piece of GRIN MMF is used to increase the wavelength separation due to its weak nonlinear effect. Finally, the residual 1.55 μm pulses are eliminated by the PMWDM3 to obtain the dual-wavelength pulses at 1.7 μm band.

As the fundamental module, the parameters of passively mode-locked fiber laser determine the design scheme of the dual-wavelength laser, therefore we make comprehensive measurements of these parameters. At first, we show the optical spectrum of the mode-locked fiber laser in Fig. 2(a), measured at a pump power of 125 mW with an output power of 5 mW. The central wavelength is 1561 nm with a 3 dB spectral bandwidth of 7.4 nm. The Kelly sidebands on the edges of spectrum indicate that the laser is operating in a soliton mode-locking state. The autocorrelation trace in Fig. 2(b) has a full width at half maximum (FWHM) width of 710 fs, corresponding to a temporal width of 502.4 fs assuming a Gaussian pulse shape. The pulse width is slightly longer than the 483.8 fs transform-limited duration, indicating that the pulses are slightly chirped. The RF spectrum in Fig. 2(c) shows a 23.75 MHz fundamental pulse repetition rate and a 72.45 dB signal-to-noise ratio (SNR), which suggests the laser has excellent stability.

Prior to entering the main amplifier, the soliton pulses are pre-amplified from 5 mW to 110 mW, resulting in a pulse energy of 4.6 nJ. The spectrum and intensity autocorrelation curve are presented in Fig. 3. Figure 3(a) shows the 3 dB spectral bandwidth of 7.5 nm centered at 1570.8 nm, corresponding to a transform-limited FWHM width of 483.9 fs, and the 10 dB bandwidth is also given as 68.7 nm. It should be noted that the spike appearing at the center of the spectrum makes the 3 dB

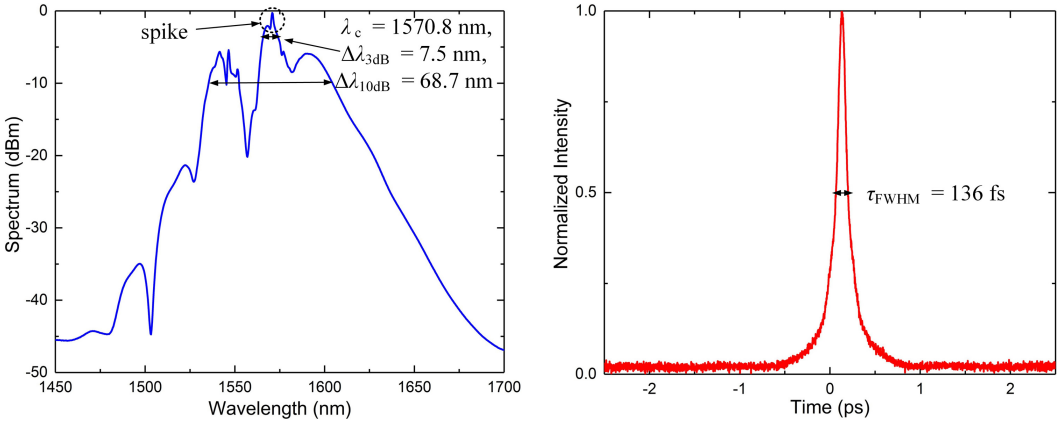

(a) (b)

Fig. 3. The parameters of pulses from the pre-amplifier. (a) Optical spectrum and (b) Intensity autocorrelation curve.

bandwidth inaccurate in describing the spectral characteristics. Figure 3(b) displays the measured intensity autocorrelation trace of the compressed pulses, showing an FWHM width of 136 fs, corresponding to a pulse width of 96.2 fs, assuming a Gaussian pulse shape. The deviation between the calculated transform limited FWHM pulse width of 483.9 fs and the measured pulse width of 96.2 fs results from the irregular spectral profile owing to the strong self-phase modulation (SPM) effect.[23,24] Moreover, the asymmetric spectral shape proves the existence of the intrapulse Raman scattering, which means the frequency shift to 1.7 μm has occurred.

To achieve a large Raman frequency shift, we increase the pulse energy to tens of nJs through a main amplifier, utilizing a 3 meter dual-cladding Er: Yb co-doped active fiber to provide high gain. Since a single mode 976 nm pump typically produces limited power of up to 1 W, a multimode pump is adopted to supply up to 9 W pump power. For balancing the central wavelengths and peak powers of the Raman peaks, we set the pump power to 6.5 W. At this power, the average power of the output pulses is 330 mW, converting to a single pulse energy of 14 nJ.

Next, the amplified pulses are directed to a 2.4 m GRIN MMF to enhance separation of the Raman peaks. Due to the weak SPM effect in GRIN MMF, the propagation of the pulses is mainly influenced by fiber dispersion, resulting in the distinct separation of Raman pulses in both time and frequency domains. The measured spectrum is shown in Fig. 4, indicating two Raman peaks located at 1641.04 nm and 1689.7 nm, respectively. The peak locations are linked to pulse energies, which can be adjusted by the pump power of the main amplifier. Nonetheless, the original signal at 1560 nm still dominates most energy, posing a significant negative effect on dual-wavelength pulses. Particularly for bioimaging applications, high pulse energy at 1560 nm would accumulate substantial heat, eventually damaging biological tissue samples.

In our laser, we employ a fast-axis blocked PMWDM3 to eliminate residual 1560 nm signals. This efficient device allows signals polarizing along the slow-axis in the range of 1640–1740 nm passing through with a designed transmittance of over 50%, while it causes an attenuation of over 20 dB for signals below 1640 nm. After passing through PMWDM3, the spectra are shown both in logarithmic and linear coordinates in Fig. 5. In comparison with Fig. 4, the central wavelengths of the Raman peaks in Fig. 5(a) remain almost constant

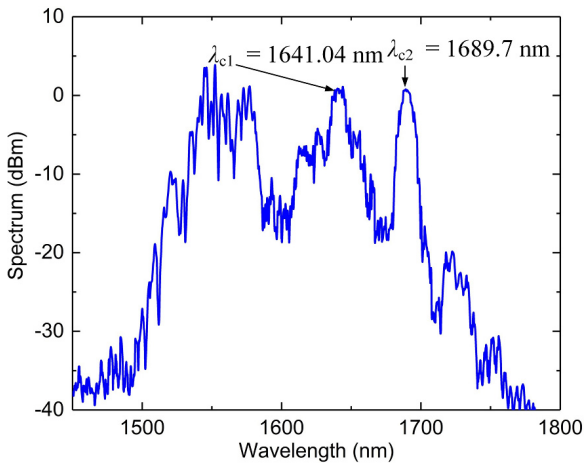

Fig. 4. The optical spectrum of pulses from the GRIN MMF.

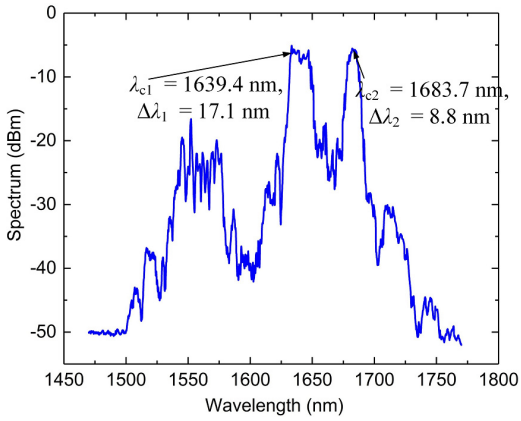

(a)

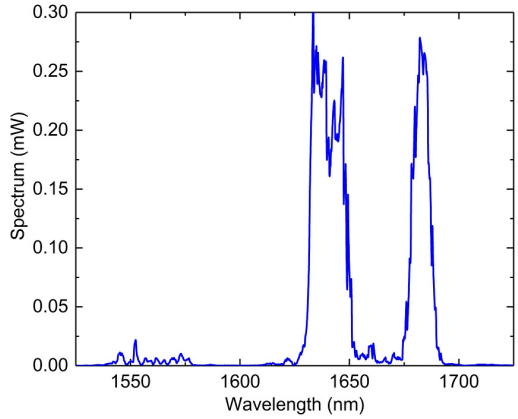

(b)

Fig. 5. The optical spectra of pulses from the PMWDM3 in (a) logarithmic and (b) linear coordinates.

at 1639.4 nm and 1683.7 nm, while the 3 dB bandwidths are 17.1 nm and 8.8 nm, respectively. The peak values of the Raman peaks are 5 dB lower than those in Fig. 4, corresponding to a transmittance of 31.6%. However, the pulses at 1560 nm are effectively attenuated by more than 20 dB, which is beneficial for bioimaging. The spectral curve plotted on the linear coordinate scale in Fig. 5(b) provides a clearer view of the PMWDM3-filtered pulses.

Figure 6 displays the autocorrelation curve of our dual-wavelength pulse laser. The curve exhibits three distinct peaks, indicating that our laser outputs two pulses per period in the time domain, corresponding exactly to the two wavelengths depicted in Fig. 5(a). The 3.8 ps interval between the secondary peak and the primary peak is mainly determined by fiber dispersions and represents the time separation between the two pulses. The FWHM width of the primary peak is 1.3 ps, corresponding to a pulse width of 920 fs assuming a Gaussian pulse shape. The 3 dB bandwidths in Fig. 5(a) correspond to the Fourier transform limit pulse widths of 220 fs and 470 fs, indicating that the dual-pulses are chirped.

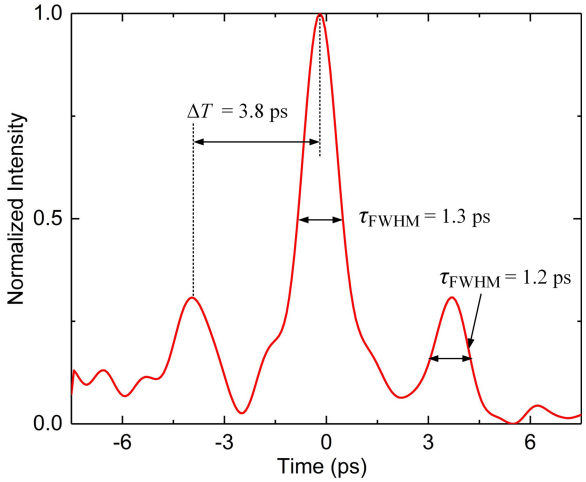

Fig. 6. The intensity autocorrelation curve of pulses from the PMWDM3.

To improve the excitation efficiency of the dye molecules in biological tissues, the pulse width usually requires to be less than 100 fs. However, a slightly extended pulse width can reduce the photobleaching. Therefore, the pulse width control is important in bioimaging. Since the dual-pulses presented in Fig. 6 are chirped, the users are able to tune pulse width conveniently by adjusting the output fiber length.

4. Discussion

For three-photon fluorescence imaging, the pulse energy and the pulse width are important parameters related to fluorescence excitation efficiency. From the result in Fig. 5, we can see that although the PMWDM3 has good performance in suppressing the signals at 1560 nm, it also leads to a significant attenuation of the Raman peaks. The tail fiber of the adopted PMWDM3 is a single mode PM fiber with a core diameter of 9.5 μm, which promises the output pulses of the fundamental mode. However, while the core diameter of the GRIN MMF is 62.5 μm, the core diameter mismatch is responsible for the low transmittance of the PMWDM3, which will be improved by replacing a multimode one. The average power of the filtered pulses is 53.64 mW, corresponding to a 2.25 nJ single pulse energy. For three-photon microscope, the pulse energy of the illumination source usually needs to reach over 10 nJ, which means we should further optimize the energy in the future. The pulse energy can be increased by dispersion management or a thulium-doped-fiber-based amplifier.[25,26]

5. Conclusions

In this paper, we introduce an innovative illumination source for dual-color three-photon fluorescence imaging which adopts a self-made all-PM passive mode-locked laser as the seed oscillator. The seed pulses undergo a two-stage amplification system, the pulse energy is increased to 14 nJ, and cascaded Raman pulses are generated. We then use GRIN MMF to adjust the Raman pulses in both the time and frequency domains, producing dual-wavelength pulses with pulse width of 920 fs and wavelength near 1.7 μm. Additionally, an all-fiber polarization-maintaining structure is utilized to ensure the output pulses are linearly polarized, meanwhile, this structure promises the environmental stability of the laser. Finally, we obtain the linearly polarized dual-color pulse sequence in a fundamental spatial mode. The dimensions of the illumination source are 24 cm$\times$ 12 cm$\times$ 45 cm, and the compact and robust structure increases its portability. Commercial components are adopted for cost reduction, which makes it easier to gain

widespread acceptance from researchers. This illumination source has tremendous potential in bioimaging research, especially in dual-color three-photon imaging and blood flow velocity measuring, which will facilitate the development of more advanced bioimaging technologies.

Acknowledgment

This work was supported by the Fundamental Research Funds for the Central Universities (HYGJXM202309).

Conflicts of Interest

The authors declare that there are no conflicts of interest relevant to this article.

References

1. W. Denk, J. H. Strickler, W. W. Webb, "Two-photon laser scanning fluorescence microscopy," *Science* **248**, 73–76 (1990).
2. D. M. Chow, D. Sinefeld, K. E. Kolkman, D. G. Ouzounov, N. Akbari, R. Tatarsky, A. Bass, C. Xu, J. R. Fetcho, "Deep three-photon imaging of the brain in intact adult zebrafish," *Nat. Meth.* **17**, 605–608 (2020).
3. N. G. Horton, K. Wang, D. Kobat, C. G. Clark, F. W. Wise, C. B. Schaffer, C. Xu, "In vivo three-photon microscopy of subcortical structures within an intact mouse brain," *Nat. Photon.* **7**, 205–209 (2013).
4. S. W. Wang, J. Liu, G. X. Feng, L. G. Ng, B. Liu, "NIR-II excitable conjugated polymer dots with bright NIR-I emission for deep in vivo two-photon brain imaging through intact skull," *Adv. Funct. Mater.* **29**, 1808365 (2019).
5. T. Y. Wang, C. Xu, "Three-photon neuronal imaging in deep mouse brain," *Optica* **7**, 947–960 (2020).
6. D. Sinefeld, F. Xia, M. R. Wang, T. Y. Wang, C. Y. Wu, X. S. Yang, H. P. Paudel, D. G. Ouzounov, T. G. Bifano, C. Xu, "Three-photon adaptive optics for mouse brain imaging," *Front. Neurosci.* **16**, 880859 (2022).
7. K. Guesmi, K. Abdeladim, S. Tozer, P. Mahou, T. Kumamoto, K. Jurkus, P. Rigaud, K. Loulier, N. Dray, P. Georges, M. Hanna, J. Livet, W. Supatto, E. Beaurepaire, F. Druon, "Dual-color deep-tissue three-photon microscopy with a multi-band infrared laser," *Light Sci. Appl.* **7**, 12 (2018).
8. H. Cheng, J. C. Zhong, P. Qiu, K. Wang, "In vivo label-free measurement of blood flow velocity symmetry based on dual line scanning third-harmonic generation microscopy excited at the 1700-nm window," *J. Innov. Opt. Health Sci.* 2350011 (2023), doi:10.1142/S1793545823500116.
9. K. Wang, W. J. Zhang, X. Q. Deng, S. Tong, H. Cheng, M. Y. Qin, L. Zheng, K. Zhao, R. Z. Zhai, Z. Q. Jia, P. Qiu, "Comparison of the emission wavelengths by a single fluorescent dye on in vivo 3-photon imaging of mouse brains," *J. Innov. Opt. Health Sci.* 2340002 (2023), doi:10.1142/S1793545823400023.
10. A. Khegai, M. Melkumov, M. Riumkin, V. Khopin, S. Firstov, E. Dianov, "NALM-based bismuth-doped fiber laser at 1.7 μm," *Opt. Lett.* **43**, 1127–1130 (2018).
11. N. K. Thipparapu, Y. Wang, S. Wang, A. A. Umnikov, P. Barua, J. K. Sahu, "Bi-doped fiber amplifiers and lasers," *Opt. Mater. Exp.* **9**, 2446–2465 (2019).
12. T. Noronen, O. Okhotnikov, R. Gumenyuk, "Electronically tunable thulium-holmium mode locked fiber laser for the 1700-1800 nm wavelength band," *Opt. Exp.* **24**, 14703–14708 (2016).
13. B. Li, M. R. Wang, K. Charan, M. J. Li, C. Xu, "Investigation of the long wavelength limit of soliton self-frequency shift in a silica fiber," *Opt. Exp.* **26**, 19637–19647 (2018).
14. K. Wang, C. Xu, "Tunable high-energy soliton pulse generation from a large-mode-area fiber and its application to third harmonic generation microscopy," *Appl. Phys. Lett.* **99**, 071112 (2011).
15. A. Zach, M. Mohseni, C. Polzer, J. W. Nicholson, T. Hellerer, "All-fiber widely tunable ultrafast laser source for multimodal imaging in nonlinear microscopy," *Opt. Lett.* **44**, 5218–5221 (2019).
16. J. W. Nicholson, A. Desantolo, W. Kaenders, A. Zach, "Self-frequency-shifted solitons in a polarization-maintaining, very-large-mode area, Er-doped fiber amplifier," *Opt. Exp.* **24**, 23396–23402 (2016).
17. R. Thouroude, H. Gilles, B. Cadier, T. Robin, A. Hideur, A. Tyazhev, R. Soulard, P. Camy, J.-L. Doualan, M. Laroche, "Linearly-polarized high-power Raman fiber lasers near 1670 nm," *Laser Phys. Lett.* **16**, 025102 (2019).
18. J. Zeng, A. E. Akosman, M. Y. Sander, "Supercontinuum generation from a thulium ultrafast fiber laser in a high NA silica fiber," *IEEE Photon. Tech. Lett.* **31**, 1787–1790 (2019).
19. H. Y. Chung, W. Liu, Q. Cao, F. X. Kärtner, G. Q. Chang, "Er-fiber laser enabled, energy scalable femtosecond source tunable from 1.3 to 1.7 μm," *Opt. Exp.* **25**, 15760–15771 (2017).

20. C. Caucheteur, D. Bigourd, E. Hugonnot, P. Szriftgiser, A. Kudlinski, M. Gonzalez-Herraez, A. Mussot, "Experimental demonstration of optical parametric chirped pulse amplification in optical fiber," *Opt. Lett.* **35**, 1786–1788 (2010).
21. Y. K. Qin, O. Batjargal, B. Cromey, K. Kieu, "All-fiber high-power 1700 nm femtosecond laser based on optical parametric chirped-pulse amplification," *Opt. Exp.* **28**, 2317–2325 (2020).
22. P. Morin, J. Dubertrand, P. B. D'Augeres, Y. Quiquempois, G. Bouwmans, A. Mussot, E. Hugonnot, "μJ-level Raman-assisted fiber optical parametric chirped-pulse amplification," *Opt. Lett.* **43**, 4683–4686 (2018).
23. S. Xing, D. M. B. Lesko, T. Umeki, A. J. Lind, N. Hoghooghi, T.-H. Wu, S. A. Diddams, "Single-cycle all-fiber frequency comb," *APL Photon.* **6**, 086110 (2021).
24. P. Steinleitner, N. Nagl, M. Kowalczyk, J. Zhang, V. Pervak, C. Hofer, A. Hudzikowski, J. Sotor, A. Weigel, F. Krausz, K. F. Mak, "Single-cycle infrared waveform control," *Nat. Photon.* **16**, 512–518 (2022).
25. F. Li, W. Zhao, Y. S. Wang, N. Wang, Q. L. Li, Y. Yang, W. L. Wen, "A large dispersion-managed monolithic all-fiber chirped pulse amplification system for high-energy femtosecond laser generation," *Opt. Laser Technol.* **147**, 107684 (2022).
26. G. Soboń, T. Martynkien, D. Tomaszewska, K. Tarnowski, P. Mergo, J. Sotor, "All-in-fiber amplification and compression of coherent frequency-shifted solitons tunable in the 1800–2000 nm range," *Photon. Res.* **6**, 368–372 (2018).